Earth and Planetary Science Letters 273 (2008) 58–67

Contents lists available at ScienceDirect

Earth and Planetary Science Letters

journal homepage: www.elsevier.com/locate/epsl

Climatic fluctuations and seasonality during the Late Jurassic (Oxfordian–Early Kimmeridgian) inferred from $\delta^{18}O$ of Paris Basin oyster shells

Benjamin Brigaud [a,b,*], Emmanuelle Pucéat [a,b], Pierre Pellenard [a,b], Benoît Vincent [c], Michael M. Joachimski [d]

[a] Université de Bourgogne, Laboratoire Biogéosciences, 6 bd Gabriel, 21000 Dijon, France
[b] CNRS, UMR 5561 Biogéosciences, 6 bd Gabriel, 21000 Dijon, France
[c] Institut Français du Pétrole (IFP) Département de Géologie-Géochimie, 1-4 Ave de Bois Préau, 92852 Rueil-Malmaison Cedex, France
[d] Institut für Geologie und Mineralogie, Universität Erlangen-Nürnberg, Schlossgarten 5, 91054 Erlangen, Germany

ARTICLE INFO

Article history:
Received 8 January 2008
Received in revised form 22 May 2008
Accepted 11 June 2008
Available online 24 June 2008

Editor: M.L. Delaney

Keywords:
oxygen isotopes
paleotemperature
carbonate
Jurassic
Paris Basin
oysters

ABSTRACT

Oxygen isotope data from biostratigraphically well-dated oyster shells from the Late Jurassic of the eastern Paris Basin are used to reconstruct the thermal evolution of western Tethyan surface waters during the Early Oxfordian–Early Kimmeridgian interval. Seventy eight oyster shells were carefully screened for potential diagenetic alteration using cathodoluminescence microscopy. Isotope analyses were performed on non-luminescent parts of shells (n=264). Intra-shell $\delta^{18}O$ variability was estimated by microsampling along a transect perpendicular to the growth lines of the largest oyster shell. The sinusoidal distribution of the $\delta^{18}O$ values along this transect and the dependence of the amplitude of variations with bathymetry suggest that intra-shell variability reflects seasonal variations of temperature and/or salinity. Average amplitudes of about 5 °C in shallow water environments and of about 2–3 °C in deeper offshore environments are calculated. These amplitudes reflect minimum seasonal temperature variation. Our new data allow to constrain existing paleotemperature trends established from fish tooth and belemnite $\delta^{18}O$ data and are in better agreement with paleontological data. More specifically, a warming trend of about 3 °C is reconstructed for oceanic surface waters during the Early to Middle Oxfordian transition, with maximum temperatures reaching 24 °C in the *transversarium* Zone (late Middle Oxfordian). From the *transversarium* Zone to the *bimmamatum* Zone, a cooling of about 7 °C is indicated, whereas from the *bimmamatum* Zone, temperatures increased again by about 7 °C to reach 24 °C in average during the *cymodoce* Zone (Early Kimmeridgian).

1. Introduction

The Jurassic climate has been commonly described as a greenhouse climate with equable global climatic conditions and warm temperatures (Frakes et al., 1992; Hallam, 1993; Sellwood and Valdes, 1997; Sellwood et al., 2000). However, recent paleontological and oxygen isotope studies provided evidence for major climatic changes during the Late Jurassic interval. More specifically, a cool episode at the Callovian–Oxfordian transition is followed by a global warming trend from the Early Oxfordian to the Kimmeridgian (Abbink et al., 2001; Dromart et al., 2003a,b; Riboulleau et al., 1998) or from the Late Oxfordian to the Kimmeridgian (Cecca et al., 2005; Lécuyer et al., 2003). There are still discrepancies between the various temperature records generated from fish tooth, belemnite and brachiopod oxygen isotope analyses. Isotopic temperatures calculated from Russian belemnites suggest a warming beginning as soon as the Early Oxfordian (Riboulleau et al., 1998) whereas fish teeth data suggest that the cool interval could have lasted up to the Late Oxfordian (Lécuyer et al., 2003). Uncertainties on the habitat of belemnites (McArthur et al., 2007) and vital effects detected in modern brachiopods (e.g. *Terebratalia transversa*, Auclair et al., 2003) have cast doubts on the reliability of the oxygen isotope composition of these organisms as a proxy for sea surface temperature (SST). In addition, although the isotopic composition of fish teeth has been shown to serve as a reliable paleotemperature proxy (Lécuyer et al., 2003; Pucéat et al., 2007; Pucéat et al., 2003), published fish tooth data are limited for this time period.

Previous studies have shown that marine bivalves precipitate their shells in oxygen isotope equilibrium with seawater (Lécuyer et al., 2004; Mook and Vogel, 1968), and their $\delta^{18}O$ values have been successfully used to reconstruct SST of past oceans (Steuber et al., 2005).

The aim of this study is to explore in detail the thermal evolution of the Oxfordian–Early Kimmeridgian interval using $\delta^{18}O$ of 54 well-preserved oyster shells recovered from biostratigraphically well-dated sections of the eastern Paris Basin. During the Late Jurassic, the Paris Basin was located at tropical latitudes (28–32° N; Thierry, 2000). Oyster shells have been recovered from three outcrops investigated in

* Corresponding author. Université de Bourgogne, UMR CNRS 5561 Biogéosciences, 6 bd Gabriel, 21000 Dijon, France.
E-mail address: benjamin.brigaud@u-bourgogne.fr (B. Brigaud).

0012-821X/$ – see front matter © 2008 Elsevier B.V. All rights reserved.
doi:10.1016/j.epsl.2008.06.015

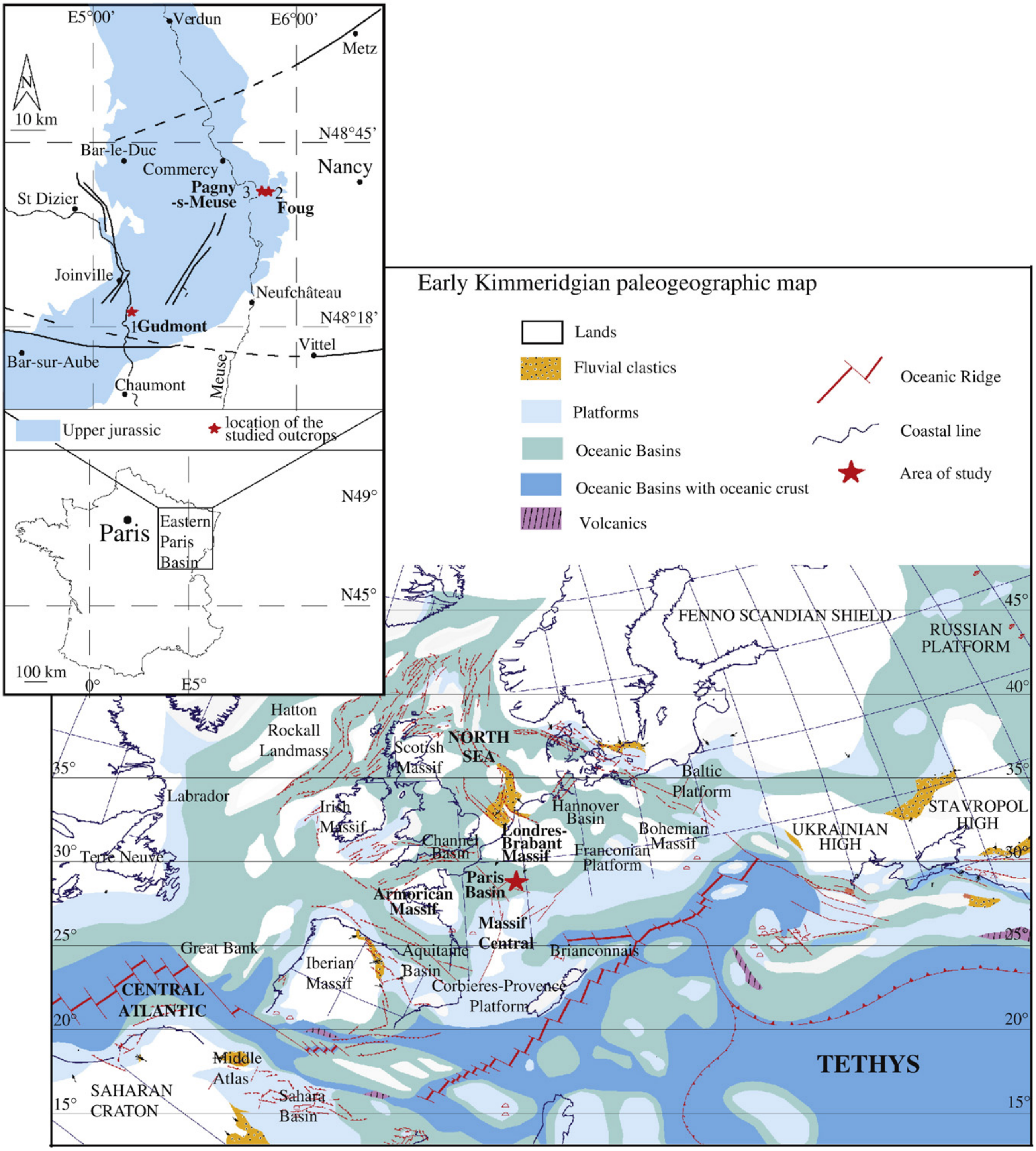

Fig. 1. Paleogeographic map of the Early Kimmeridgian (Thierry, 2000) of the Paris Basin and location of the three studied sections in the Eastern part of the Paris Basin (Lorraine Region): 1—Gudmont, 2—Foug and 3—Pagny-sur-Meuse.

detail in previous studies that allow to constrain the stratigraphic position of the samples with a time resolution higher than an ammonite biozone and to define the depositional environment of the samples at water depths of no more than 50 m. Oysters tolerate a large range of salinity (Surge et al., 2001), and therefore can live in water with an oxygen isotope composition which differs to that of open marine seawater. Therefore, the living environment of oysters has to be carefully constrained prior to any isotopic analyses. A detailed sedimentological study of the sections yielding the oyster shells we used, replaced in a regional paleoenvironmental setting, reveals that all of the oysters analysed in our study lived in an open marine environment and are therefore suitable for the paleotemperature reconstruction. In addition to secular sea surface water temperature changes, we focus on seasonal variations of paleotemperatures during the Oxfordian–Early Kimmeridgian period, through microsampling and analyses of oxygen isotope ratios along a transect perpendicular to the growth lines of the largest oyster shell. Finally, comparison of the $\delta^{18}O$ data reported in this study with previously published

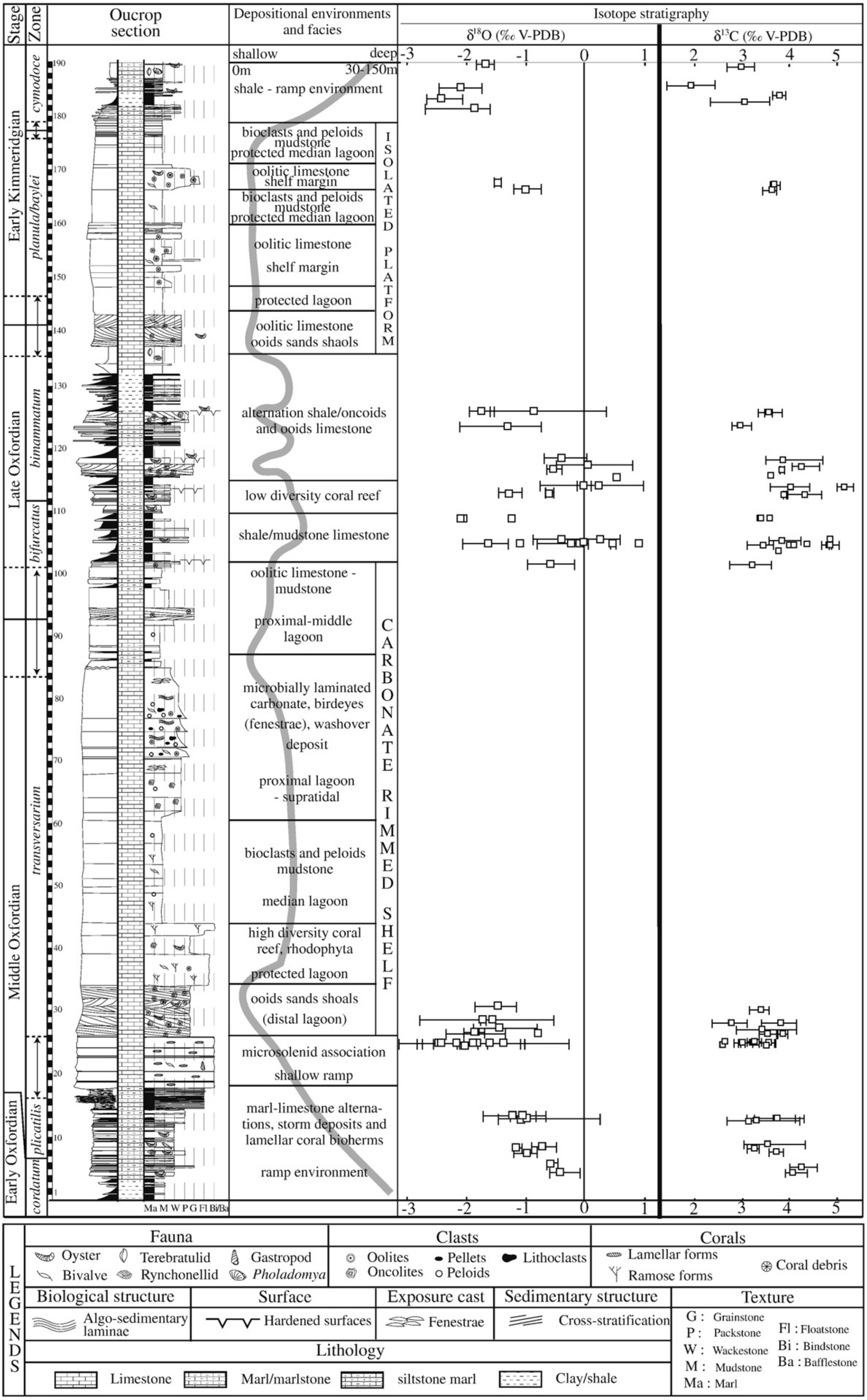
Stage
Zone
Oucrop section
Depositional environments and facies
Isotope stratigraphy
δ18O (‰ V-PDB)
δ13C (‰ V-PDB)
shallow
deep
0m
30-150m
Early Kimmeridgian
Late Oxfordian
Middle Oxfordian
Early Oxfordian
cymodoce
planula/baylei
bimammatum
bifurcatus
transversarium
plicatilis
cordatum
shale - ramp environment
bioclasts and peloids mudstone protected median lagoon
oolitic limestone shelf margin
bioclasts and peloids mudstone protected median lagoon
oolitic limestone
shelf margin
protected lagoon
oolitic limestone ooids sands shaols
ISOLATED PLATFORM
alternation shale/oncoids and ooids limestone
low diversity coral reef
shale/mudstone limestone
oolitic limestone - mudstone
proximal-middle lagoon
microbially laminated carbonate, birdeyes (fenestrae), washover deposit
proximal lagoon - supratidal
bioclasts and peloids mudstone
median lagoon
high diversity coral reef, rhodophyta
protected lagoon
ooids sands shoals (distal lagoon)
CARBONATE RIMMED SHELF
microsolenid association
shallow ramp
marl-limestone alternations, storm deposits and lamellar coral bioherms
ramp environment
Ma M W P G Fl Bi/Ba
LEGENDS
Fauna
Oyster
Terebratulid
Gastropod
Bivalve
Rynchonellid
Pholadomya
Clasts
Oolites
Pellets
Lithoclasts
Oncolites
Peloids
Corals
Lamellar forms
Ramose forms
Coral debris
Biological structure
Algo-sedimentary laminae
Surface
Hardened surfaces
Exposure cast
Fenestrae
Sedimentary structure
Cross-stratification
Texture
G : Grainstone
P : Packstone
W : Wackestone
M : Mudstone
Ma : Marl
Fl : Floatstone
Bi : Bindstone
Ba : Bafflestone
Lithology
Limestone
Marl/marlstone
siltstone marl
Clay/shale

$\delta^{18}O$ data from belemnite rostra, fish teeth, and brachiopod shells is used to discuss the relevance of these different materials for SST reconstructions.

This study contributes to a better understanding of the Late Jurassic climate by providing a new detailed paleotemperature curve for the Oxfordian–Early Kimmeridgian interval.

2. Geological and paleoenvironmental setting

Oyster shells were sampled in three complementary outcrops from the eastern part of the Paris Basin: Foug, Pagny-sur-Meuse and Gudmont (Fig. 1). Sedimentology and biostratigraphy of the sections are well-constrained by previous studies (Carpentier et al., 2007; Debrant-Passard et al., 1980; Enay and Boullier, 1981; Olivier et al., 2004; Vincent et al., 2006) (Fig. 2) and enabled us i) to constrain the stratigraphic position of the samples with a time resolution higher than an ammonite biozone, and ii) to define precisely the depositional environment of each sample in order to estimate paleobathymetry.

During the Oxfordian and the Early Kimmeridgian, the Paris Basin was an epicontinental sea (Thierry, 2000) located at subtropical latitudes (28–32° N), open to the Atlantic, Tethys, and Northern oceans (Fig. 1). The upper part of the Early Oxfordian is mainly composed of marl–limestone alternations that were deposited along a ramp dipping southward from the London–Brabant landmass. The abundance of carbonate beds increases upward from the underlying Callovian–Oxfordian clayey deposits, which reveal a progressive evolution from an outer to mid-ramp environment (Vincent et al., 2006). Hydrodynamic evidences such as erosional furrows suggest that water depth was comprised between fair weather and storm wave base (Tucker and Wrigth, 1990). Additional evidence is provided by coral associations with *Microsolena* and *Dimorpharaea* which indicate water depths of around 50 m (Lathuilière et al., 2005). As ammonites are abundant, a subzone ammonite resolution is reached in these deposits (Enay and Boullier, 1981).

In the Middle Oxfordian, a rimmed shelf with a diversified facies was developed in the North-East Paris Basin. Three main depositional environments are recognized: i) a typical platform barrier environment is indicated by abundant ooids, oncoids, pellets, oysters, bryozoans and gastropods (Vincent et al., 2006); ii) the barriers delineated a protected lagoon with highly diverse coral reefs and with a mudstone inter-reef facies, which define the second depositional environment (Olivier et al., 2004). Rhodophyta associated with corals suggest a bathymetry lower than 30 m; iii) a more proximal lagoon setting with short tide-related episodic subaerial exposure (Vincent et al., 2006) is characterized by an association of laminated mudstone (stromatolites and tidal-flat laminations) with fenestral structures, and ostracod-rich facies. Some storm events are recorded within the latter environment by the occurrence of coarse-grained lithoclastic and bioclastic layers interbedded in the micritic limestones. Ammonites reported in inter-reefs environments ascribe it to the *transversarium* Zone (Enay and Boullier, 1981).

An abrupt lithological change occurred at the Middle/Late Oxfordian boundary with the appearance of mixed carbonate/terrigenous sediments. Above the boundary, the presence of ammonites, identifying the *bifurcatus* Zone (Enay and Boullier, 1981), in clayey sediments clearly indicates a deepening, but the occurrence of coral patch reefs indicates that water depths were 50 m at most (Lathuilière et al., 2005). Above these sediments, two oolitic limestone units (3 m) with cross-bedding and abundant oysters, gastropods, bryozoans indicate shallowing upward phases.

In the Kimmeridgian, carbonate production resumed in the study area with shallow water sediments including ooid grainstones (sandwaves) being deposited. The ooid facies are overlain by lagoonal micritic limestones displaying scarce storm washovers. The upper part of the Early Kimmeridgian indicates another deepening event. The limestones display an increasing number of tempestite deposits including HCS (hummocky cross stratification), and are replaced by shale deposits with oysters, brachiopods and ammonites which indicate the *cymodoce* Zone (Vincent, 2001). The clay formation suggests a lower offshore environment, possibly more than 50 m deep.

All along the investigated interval, there is no sedimentological evidence for significant freshwater influx and related geographically extended significant decrease of salinity in the study area. The only existing exposed landmass is the London–Brabant massif located 150 km to the north. Since this massif is not so extended (Fig. 1) and at that time displays poorly expressed reliefs, one can expect limited drainage basins and thus restricted river influx to the ocean. Most of the flux is oriented to the north as illustrated by the fluvial clastics recorded in the North Sea (Fig. 1), which are moreover the results of focused fluxes coming from various exposed landmasses bordering the sea (Fig. 1). There is not any fluvial record to the south of the London–Brabant in the Oxfordian–Kimmeridgian. Few non-perennial islands existed during the interval, as illustrated by few poorly evolved paleosoils and lignite layers (Vincent, 2001), and rainfalls may have locally decrease the salinity in the immediate vicinity of such islands (Vincent et al., 2006). However, such a phenomenon was probably very restricted in both space and time, and even geographically non-significant. We therefore consider that there was no large variation of salinity along the studied stratigraphic interval.

3. Materials and methods

A total of 78 oyster shells were sampled along the studied stratigraphic interval. Part of the shells was investigated using scanning electron microscopy (SEM) in order to identify diagenetic recrystallisation. Only the calcitic foliated structure of the oyster shells seems well-preserved (Appendix A). In addition, thick polished sections of all oyster shells were examined using cathodoluminescence (CL) microscopy. CL analyses were carried out on a 8200MKII Technosyn cathodoluminescence coupled to an Olympus microscope. Luminescent and non-luminescent areas of each shell section were accurately mapped in order to be able to sample the non-luminescent parts of the shells for stable isotope analysis. CL reveals 4 types of alteration characterized by an orange luminescence (Appendix A): (i) thin delaminations (about 1 μm thick), ii) parts of shells that recrystallized to sparite, iii) microfractures and iiii) microborings filled with luminescent micrite. After CL studies, analyses of oxygen and carbon isotopes ($n=264$) were carried out on calcite drilled from non-luminescent areas of 54 well-preserved shells. On average, 4 subsamples have been analysed from every shell. One oyster shell (sample 11, *Deltoideum delta*) was large enough to measure 68 subsamples along a transect perpendicular to the growth lines with a 0.1 mm sampling resolution (Appendix A). In order to compare the isotopic signature of luminescent and non-luminescent calcite, two luminescent oyster shells and three luminescent grainstone samples were analyzed as well.

Isotope analyses were performed at the Institute of Geology and Mineralogy, University of Erlangen-Nuremberg. Calcite powders were reacted with 100% phosphoric acid at 75 °C using a Kiel III online carbonate preparation line connected to a ThermoFinnigan 252 masspectrometer. All isotopic values are reported in the standard δ-notation in per mil relative to V-PDB (Vienna Pee Dee Belemnite) by assigning a $\delta^{13}C$ value of +1.95‰ and a $\delta^{18}O$ value of −2.20‰ to NBS19. Reproducibility was checked by replicate analysis of laboratory

Fig. 2. Sedimentological log, depositional environment, facies, paleobathymetry and isotope stratigraphy ($\delta^{18}O$ and $\delta^{13}C$ values) of the Oxfordian–Early Kimmeridgian from the Eastern Paris Basin. This sedimentological log is a composite section of the studied intervals at Foug (0–25 m), Pagny-sur-Meuse (25–172 m) and Gudmont (172–190 m). Bi-directional arrows correspond to uncertainties on the dating of biozonation boundaries.

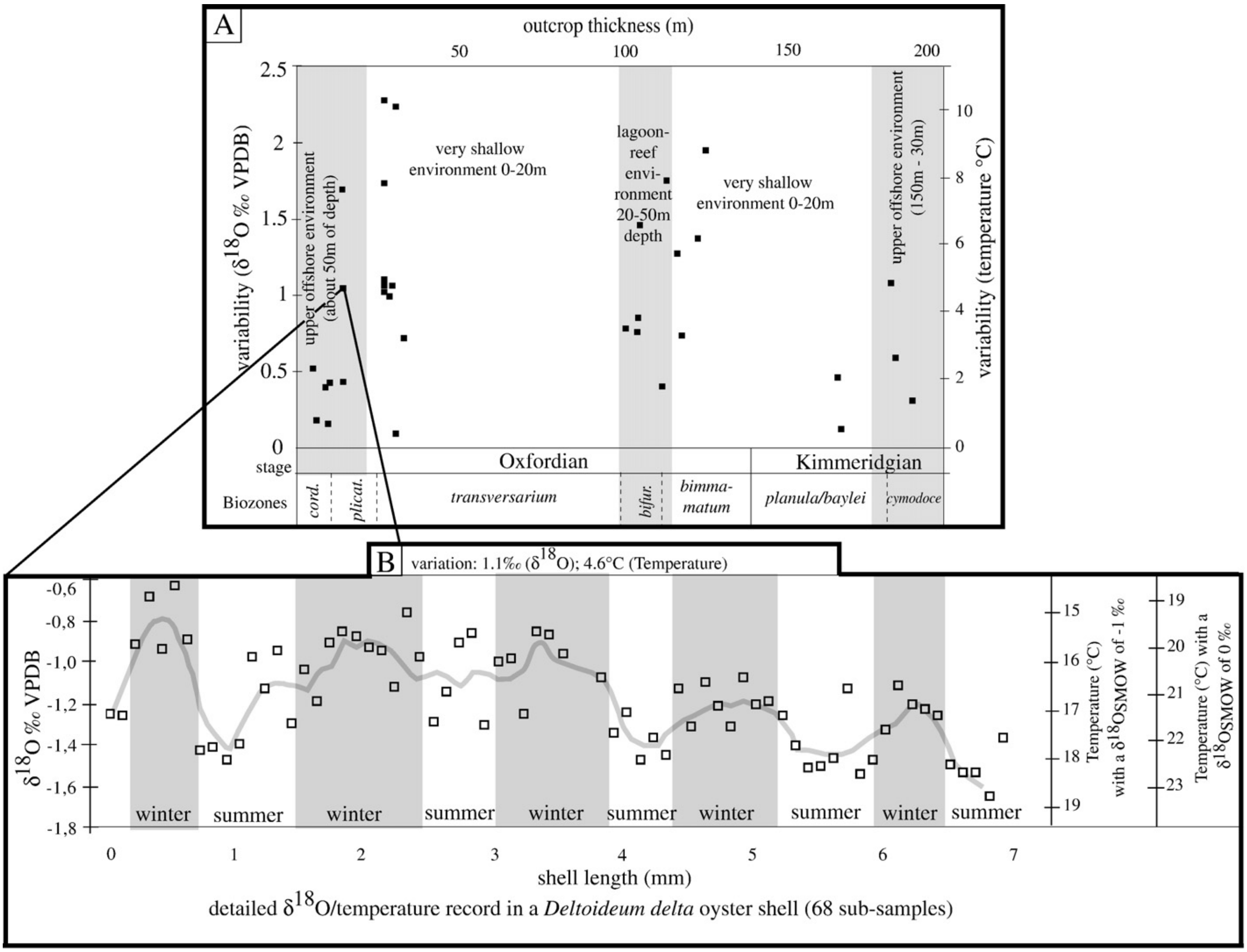

Fig. 3. A—Intra-shell variability evolution during Oxfordian and Kimmeridgian stage. Intra-shell variability was obtained on 33 oyster shells that have more than 2 samples and represents the difference between maximum and minimum $\delta^{18}O$ values within a single oyster shell. Intra-shell average variability for the five intervals: *cordatum–plicatilis* Zones (0.6‰–2.6 °C), *transversarium* Zone (1.2‰–5.6 °C), *bifurcatus* Zone (0.8‰–3.6 °C), *bimmamatum* Zone (1.4‰–6 °C) and *baylei–cymodoce* Zones (0.5‰–2.4 °C). Correspondence with temperature is based on the equation of Anderson and Arthur (1983). The variability recorded in oyster shells depends on bathymetry: it is low in deeper environments and maximal in shallower environments. B—Intra-shell transect carried out on *Deltoideum delta* oyster (sample no. 11). 68 micro-samples of calcite powder have been sampled perpendicularly to the growth lines of the specimen. The running mean of $\delta^{18}O$ values (grey line) displays a sinusoidal pattern which suggests that seasonal temperature variations have been recorded.

standards and was ±0.05‰ (1σ) for oxygen isotopes and ±0.02‰ (1σ) for carbon isotopes.

4. Results

4.1. Oxygen isotopes

The oxygen isotope composition of the 264 non-luminescent oyster samples varies between −3.1 and +1.0‰ (Fig. 2 and Appendix B). The values display a relatively large variability both between several oysters from the same stratigraphic bed and within a single oyster shell (Fig. 2). The intra-shell variability has been quantified using the difference between maximum and minimum $\delta^{18}O$ values of oyster shells that have more than 2 isotope analyses (Fig. 3).

The intra-shell variability evolves through the Oxfordian–Early Kimmeridgian interval (Fig. 3). The lowest variability is recorded during the Early to early Middle Oxfordian (0.6‰ on average for the *cordatum–plicatilis* Zones), during the early Late Oxfordian (0.8‰ on average for the *bifurcatus* Zone) and during the Early Kimmeridgian (0.5‰ on average for the *baylei–cymodoce* Zones). The highest variability is recorded during the Middle Oxfordian (1.2‰ on average for the *transversarium* Zone) and during the Late Oxfordian (1.4‰ on average for the *bimmamatum* Zones). The oxygen isotope values within single oyster shells are not randomly distributed. The transect that was drilled perpendicularly to the growth lines of the larger oyster shell display a sinusoidal distribution of the $\delta^{18}O$ values (Fig. 3B). $\delta^{18}O$ values of this early Middle Oxfordian oyster shell (*plicatilis* Zone, sample 11, *D. delta*) range from −1.7 to −0.6‰ (Fig. 3B) with a variability of 1.1‰ (n=68).

Despite the large variability displayed in the oxygen isotope values, the $\delta^{18}O$ values of non-luminescent oyster shells exhibit a trend along the studied stratigraphic time interval. The Early Oxfordian (*cordatum* Zone) and early Middle Oxfordian (*plicatilis* Zone) oysters are characterized by high $\delta^{18}O$ values with an average of −1.1‰. $\delta^{18}O$ values decrease to average values around −1.8‰ in the Middle and late Middle Oxfordian (*transversarium* Zone; Fig. 2). $\delta^{18}O$ values of Late Oxfordian (*bifurcatus* and *bimmamatum* Zone) oyster shells are about 1.5‰ higher with average values around −0.6‰. From the Late Oxfordian to Early Kimmeridgian, $\delta^{18}O$ values decrease to −2.0‰ in the *cymodoce* Zone (Fig. 2).

4.2. Carbon isotopes

The carbon isotope composition of the oyster shells varies between 1.4 and 5.4‰ (Figs. 2 and 4, and Appendix B). Intra-shell variability is lower than 2‰ along the stratigraphic interval. The Early Oxfordian and Middle Oxfordian shells are characterized by relatively high δ^{13}C values of 3.6‰ on average. A decrease occurs up to the Middle Oxfordian with the lowest average values of 3.3‰ observed in the late Middle Oxfordian (*transversarium* Zone; Fig. 2). The δ^{13}C values increase by about 0.8‰ to reach a maximum of 4‰ on average during the Late Oxfordian (*bifurcatus* Zone) and decrease again from the Late Oxfordian to Early Kimmeridgian to an average value of 3.0‰ in the *cymodoce* Zone (Fig. 2).

5. Discussion

Oyster shells are not often used for paleotemperature reconstructions because they tolerate a large range of salinity (Surge et al., 2001). This can be an obstacle to paleotemperature reconstruction, as the oxygen isotope composition of the water in which they live can differ from that of the open ocean. However, there is no evidence in the studied sections for important salinity variations all along the studied stratigraphic interval (cf. Section 2). This allows us to use oyster shell δ^{18}O as a temperature proxy. Since marine molluscs precipitate their shells in oxygen isotope equilibrium with seawater, the oxygen isotope composition of shell calcite has been used to reconstruct seawater paleotemperatures (e.g. Steuber et al., 2005). Temperatures were calculated using the equation given by Anderson and Arthur (1983):

$$T = 16\text{–}4.14\left(\delta^{18}\mathrm{O}_{\mathrm{calcite}}-\delta^{18}\mathrm{O}_{\mathrm{seawater}}\right) + 0.13\left(\delta^{18}\mathrm{O}_{\mathrm{calcite}}-\delta^{18}\mathrm{O}_{\mathrm{seawater}}\right)^2$$

where T is the temperature in degree Celsius, $\delta^{18}\mathrm{O}_{\mathrm{calcite}}$ the oxygen isotope composition of calcite (relative to V-PDB) and $\delta^{18}\mathrm{O}_{\mathrm{seawater}}$ the oxygen isotope ratio of seawater (relative to V-SMOW).

Paleotemperature calculation requires an assumption for the δ^{18}O of Jurassic seawater. The oxygen isotope composition of surface seawater is dependent on (i) the evolution of continental ice sheets that modifies the δ^{18}O of the global ocean by storing preferentially ^{16}O in high latitude ice caps, (ii) the local evaporation/precipitation ratio, and, (iii) continental runoff. The Jurassic has often been considered as an "ice-free" time period due to the absence of glacial deposits during its major part (Frakes et al., 1992; Hallam, 1993; Sellwood and Valdes, 1997; Sellwood et al., 2000). For an ice-free period, a seawater δ^{18}O value of −1‰ is generally assumed (Shackleton and Kennet, 1975). However, the Paris Basin was located at subtropical latitudes that may have been characterized by intensified evaporation, resulting in increased salinity and a higher δ^{18}O value of subtropical surface waters (Lécuyer et al., 2003; Pucéat et al., 2003; Roche et al., 2006). Both the dominance of evaporation over precipitation and the potential occurrence of limited ice sheets during the Jurassic led some authors to use a δ^{18}O value of 0‰ for the calculation of SST (e.g. Lécuyer et al., 2003). Consequently, we use a δ^{18}O of 0‰ for Jurassic surface waters in the Paris Basin. With this assumption, calculated temperatures are about 4 °C lower in comparison to paleotemperatures calculated with a seawater δ^{18}O value of −1‰.

5.1. Seasonal variation of temperature

The intra-shell δ^{18}O variability recorded in individual oyster shells translates into 0.5 to 10 °C temperature changes, if explained exclusively by temperature variations (Figs. 3 and 5). The intra-shell variability reveals minimal values during the Early Oxfordian to early Middle Oxfordian (2.6 °C on average for the *cordatum–plicatilis* Zones), early Late Oxfordian (3.6 °C on average for the *bifurcatus* Zone) and Early Kimmeridgian (2.4 °C on average for the *baylei–cymodoce* Zones), and maximal values (up to 10 °C; Fig. 3A) during the late Middle Oxfordian (5.6 °C on average for the *transversarium* Zone) and late Late Oxfordian (6 °C on average for the *bimmamatum* Zone) The δ^{18}O values of the oyster shell that was sampled with 0.1 mm resolution display a sinusoidal pattern (Fig. 3B). The consistency of the amplitude of variations within this single oyster shell as well as the sinusoidal pattern suggests that seasonal temperature and/or salinity variations controlled intra-shell δ^{18}O variations.

If explained exclusively by temperature, the densely sampled oyster *D. delta* (sample 11), that lived in a reconstructed water depth less than 50 m (Lathuilière et al., 2005), shows seasonal temperature variations between 1.5 and 3 °C, with winter temperatures typically between about 19 and 21 °C, and summer temperatures typically between about 22.5 and 23.5 °C (Fig. 3B). Interestingly, the evolution of the intra-shell δ^{18}O variability during the Oxfordian to Early Kimmeridgian interval coincides with variations of the estimated paleobathymetry (Fig. 3A). Intra-shell variability is low in the deepest marine environments (during *cordatum*, *plicatilis* and *cymodoce* Zones; Fig. 3A), which corresponds to that recorded on the densely sampled oyster shell *D. delta*, and relatively high (up to 10 °C and 5–6 °C on average; Fig. 3A) in very shallow environments. The good correspondence between bathymetry and intra-shell variability in δ^{18}O suggests as well a seasonal temperature and/or salinity control on the δ^{18}O variability within each oyster. As 4 analyses in average have been performed within a single oyster, only part of the whole seasonal temperature or salinity variations would be recorded by intra-shell δ^{18}O variability. As reduction or cessation of shell growth may have occurred during seasonal extremes of temperature or

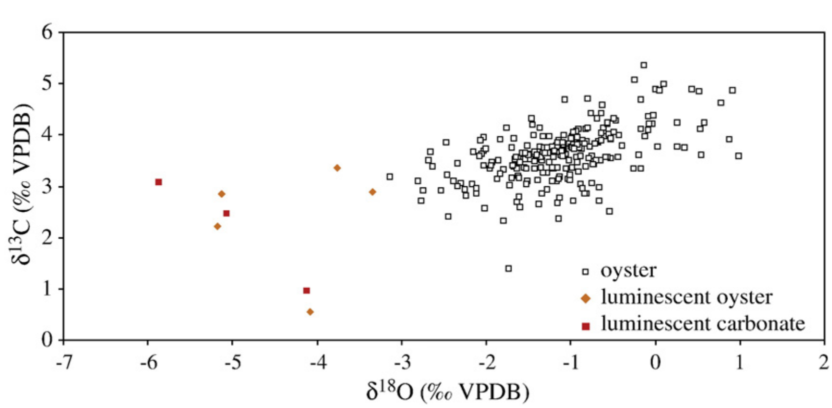

Fig. 4. Carbon versus oxygen isotope values of non-luminescent oysters, luminescent oysters and luminescent grainstones. Luminescent oysters and luminescent grainstones delineate an area affected by diagenesis with low oxygen isotopic values (<−3.1‰). The oxygen isotope composition of the 264 non-luminescent oyster samples varies between −3.1 and +1.0‰ and the carbon isotope between 1.4 and 5.4‰.7

salinity and as seasonal extremes are probably reduced by samples that can average about one month of shell growth, estimates of seasonality from the more densely sampled oyster shell (Fig. 3B) should also be considered as minimum estimates.

In addition, seasonal variations in $\delta^{18}O_{seawater}$ as consequence of seasonal changes in surface water salinity may result in an over- or underestimation of the amplitude of seasonal temperature variations. In a temperate to arid climate, a covariance of salinity, $\delta^{18}O_{seawater}$ and SST is observed since the warm season is associated with elevated evaporation, higher salinity and higher $\delta^{18}O$ values of surface waters. In contrast, a monsoonal climate system is characterized by an inverse covariance of SST and both salinity and $\delta^{18}O_{seawater}$ as the warm season is associated with more humid conditions leading to a decrease in surface water salinity and $\delta^{18}O_{seawater}$. Since the Tethys is assumed to have been associated with a monsoonal circulation during the Jurassic period (Weissert and Mohr, 1996), the calculated seasonal temperature range would be overestimated as lower salinities and lower $\delta^{18}O_{seawater}$ would be associated with higher temperatures during the humid warm season and as salinity and $\delta^{18}O_{seawater}$ would increase during the drier and cooler winter months.

Seasonal $\delta^{18}O_{seawater}$ variations are difficult to quantify for the Jurassic time period. We use sea surface salinity variations in modern tropical surface waters in comparable environmental settings to correct the Jurassic $\delta^{18}O$ signals, as a first-order approach. The Gulf of Mexico, the South China Sea, and the East Florida platform are possible environmental analogues to the Paris Basin, as they represent epicontinental seas located at 25–30° N and display an inverse covariance of SST and salinity and $\delta^{18}O_{seawater}$. In these modern environments, the amplitude of seasonal variations in surface water salinity ranges from 0.2‰ (East Florida) to 1.8‰ (China Sea); (Levitus et al., 1994 and Table 1). By using the relationship between $\delta^{18}O_{seawater}$ and salinity established for the Gulf Stream and Gulf of Mexico ($\delta^{18}O_{seawater}=0.11S-3.15$; Fairbanks et al., 1992), the seasonal changes in salinity correspond to changes in $\delta^{18}O_{seawater}$ of 0.03 to 0.2‰, respectively. Assuming maximum seasonal variations in $\delta^{18}O_{seawater}$ of 0.2‰, summer temperatures calculated from the oxygen isotope composition of the oyster shells are lowered by up to 0.5 °C, whereas the winter temperatures increase by up to 0.5 °C. The amplitude of the seasonal temperature variations calculated with a constant $\delta^{18}O_{seawater}$ would therefore be overestimated by up to about 1 °C. It is important to note that seasonal variations in $\delta^{18}O_{seawater}$ have a pronounced effect only on shallow surface waters, which are directly affected by the precipitation and evaporation. When corrected for salinity variations, the amplitude of seasonal temperature variations derived from maximum intra-shell $\delta^{18}O$ variations would be reduced from 10 °C to 9 °C. The average intra-shell temperature variability of about 6 °C can be reduced to 5 °C.

At present, seasonal variations of surface water temperature in tropical latitudes (≈30° N) vary between 5.5 °C and 13 °C (5.5 °C in the Gulf of Mexico, 12 °C on the east Florida platform and 13 °C in the China Sea; Levitus and Boyer, 1994 and Table 1). Seasonal temperature variations in 50 m water depth at 30° N are on average 5 °C (3 °C in the Gulf of Mexico, 4.5 °C in the Mediterranean sea and 8 °C in the China Sea); (Levitus and Boyer, 1994 and Table 1). Minimum estimates of seasonal temperature variations recorded in the Oxfordian were thus within or slightly lower than the modern seasonal temperature range.

5.2. Late Jurassic climate change

Despite the variability in $\delta^{18}O$ described above, a 0.25 million year running mean allows to reconstruct the thermal evolution of western Tethyan seawater during the Oxfordian–Kimmeridgian period (Fig. 5). A temperature increase of about 6 °C is calculated from the Early to the Middle Oxfordian, with maximum temperatures reaching 24 °C in the *transversarium* Zone (Fig. 5). During the *bifurcatus–bimmamatum* Zones, a cooling of about 7 °C is identified with average temperatures being around 17 °C. The Early Kimmeridgian is characterised by another temperature increase by about 8 °C to reach a maximum of 25 °C during the *cymodoce* Zone (Fig. 5). However, it is questionable whether the temperature variations reflect solely climatic changes or are in part due to changes in bathymetry. Sedimentological as well as paleontological evidences point to change in bathymetry from paleodepths of 20 m or less for the shallowest environments to paleodepths of about 50 m for the deepest environments (Fig. 3A). In modern environments, the vertical thermal change in the first 50 m of the water column is about 2 °C (Levitus and Boyer, 1994 and Table 1). For the Jurassic period, previous studies (Picard et al., 1998) have proposed a temperature decrease of 3.5 °C in the first 50 m of the water column based on $\delta^{18}O$ values of fish tooth apatite and brachiopod calcite. A thermal gradient of 3 °C for a water depth of 50 m would reduce the inferred warming trend recorded in the *cordatum* to the *transversarium* Zone from 6 °C to 3 °C with minimal thermal of 21 °C in the *cordatum* Zone, whereas the warming trend from the *bimmamatum* to the *cymodoce* Zone would increase from 8 °C to 11 °C (Fig. 5). During the Late Oxfordian and Early Kimmeridgian, an 11 °C warming appears unrealistic for a subtropical region, but if we consider a 1‰ decrease of ocean oxygen isotope composition due to a waning of potential polar ice as suggested during Callovian–Oxfordian transition (Dromart et al., 2003b) the warming would be reduced to 7 °C. The assumption of polar ice sheets is

Table 1
Temperatures and salinities data in few modern environments

Locality		Gulf of Mexico (23.5°N–89.5°W)			China (29.5°N–125.5°E)			Florida (30°N–78.22°W)		
Water depth		0 (m)	50 (m)	100 (m)	0 (m)	50 (m)	100 (m)	0 (m)	50 (m)	100 (m)
Temp. (°C)	Min.	23.5	23	21.2	16	16	16.5	22.5	22.5	22
	Max.	29	26	22.6	28	24	19.5	29	27	24
	Average	26.25	24.5	21.9	22	20	18	25.75	24.75	23
	Amplitude	5.5	3	1.4	12	8	3	6.5	4.5	2
Salinity (‰)	Min.	36.2	36.33	36.36	32.4	34.05	34.44	36.02	36.25	36.42
	Max.	36.55	36.42	36.45	34.2	34.35	34.58	36.25	36.4	36.54
	Average	36.38	36.38	36.40	33.3	34.2	34.51	36.135	36.33	36.48
	Amplitude	0.35	0.09	0.09	1.8	0.3	0.14	0.23	0.15	0.12
$\delta^{18}O$-‰	Min.	0.83	0.85	0.85	0.41	0.60	0.64	0.81	0.84	0.86
	Max.	8.87	0.86	0.86	0.61	0.63	0.66	0.84	0.86	0.87
	Average	0.85	0.855	0.855	0.51	0.615	0.65	0.825	0.85	0.865
	Amplitude	0.04	0.01	0.01	0.20	0.03	0.02	0.03	0.02	0.01

Annual minimum, maximum temperatures and salinities at 0 m, 50 m and 100 m deep from the Gulf of Mexico, China and Florida. Data from Levitus and Boyer (1994) and Levitus et al. (1994), available at http://ingrid.ldeo.columbia.edu/SOURCES/.LEVITUS94/.
Average temperature, amplitude of seasonal temperature and salinity variations are presented. Minimum and maximum $\delta^{18}O$ of seawater are calculated from the $\delta^{18}O_{seawater}$–salinity relationship established for the Gulf Stream and Gulf of Mexico ($\delta^{18}O_{seawater}=0.11S-3.15$; (Fairbanks et al., 1992).

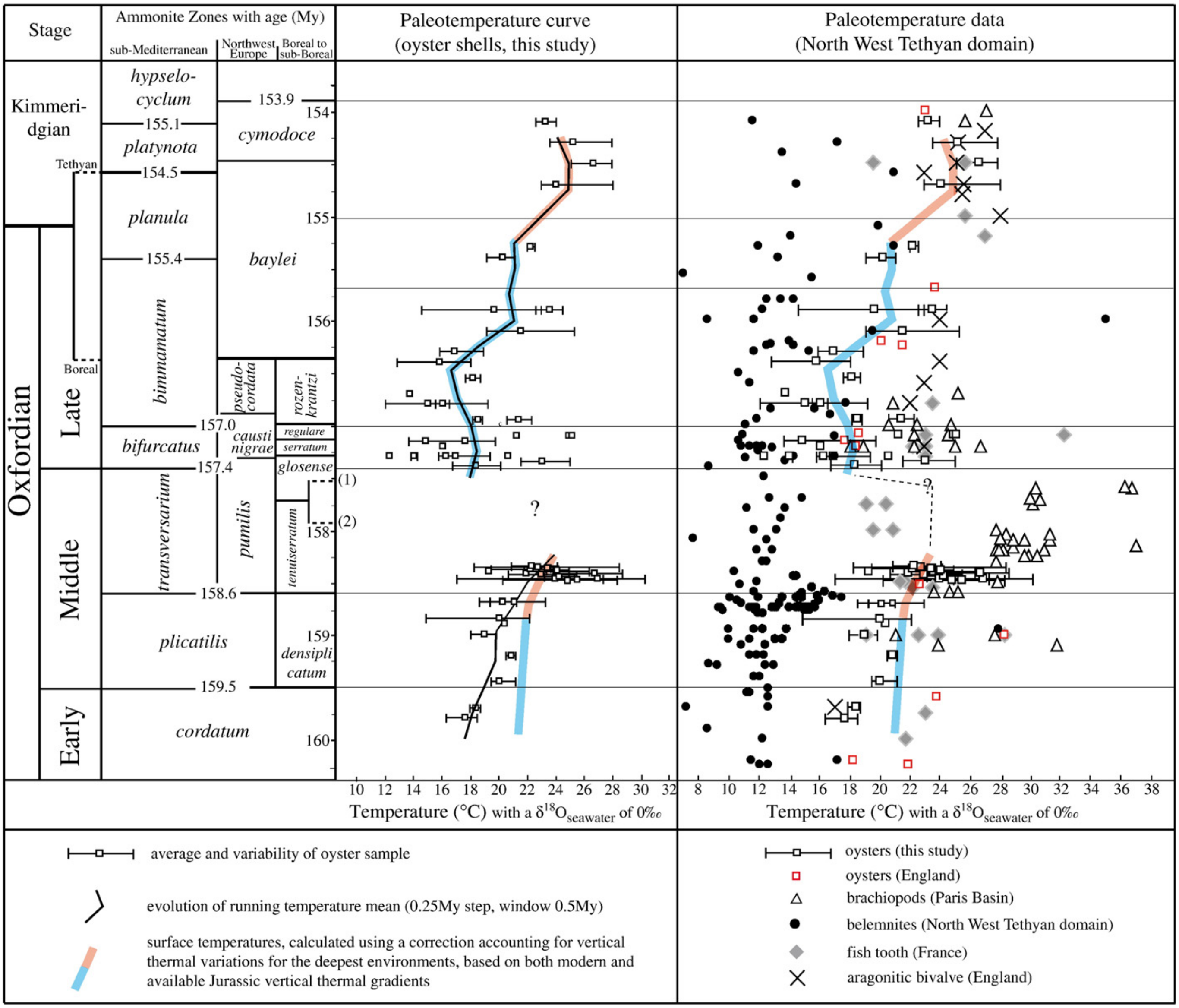

Fig. 5. Evolution of mean seawater temperatures estimated from Oxfordian–Early Kimmeridgian oyster shell $\delta^{18}O$ values. Absolute ages are derived from the geological timescale (Gradstein et al., 2004). Oxfordian ammonite biozone correlation between Sub-Mediterranean, Northwestern Europe and Boreal, Sub-boreal after (Głowniak, 2005; Głowniak and Wierzbowski, 2007; Gradstein et al., 2004; Matyja and Wierzbowski, 1998; Matyja et al., 2006). (1) Position of the *tenuiseratum/glosense* boundary after Głowniak (2005), Głowniak and Wierzbowski (2007), Matyja and Wierzbowski (1998), Matyja et al. (2006). (2) Position of the *tenuiseratum/glosense* boundary after Gygi et al. (1998), Matyja and Wierzbowski (1997), Pearce et al. (2005), Schweigert and Callomon (1997). Paleotemperatures were calculated using the temperature equation of Anderson and Arthur (1983), and with a $\delta^{18}O_{seawater}$ of 0‰ except for belemnites for which a $\delta^{18}O_{seawater}$ of −1‰ was used, for deeper marine environments and higher latitudes. The black thin curve is a running mean (0.25 Ma step, time window of 0.5 Ma). The bold colour curve includes a correction for changes in bathymetry throughout the Oxfordian–Kimmeridgian interval. Comparison of our results with isotopic temperatures available from literature, inferred from the $\delta^{18}O$ of brachiopods (Carpentier et al., 2006; Picard et al., 1998), belemnites (Jenkyns et al., 2002; Jones et al., 1994; Podlaha et al., 1998; Wierzbowski, 2002; Wierzbowski, 2004), oysters (Jenkyns et al., 2002) and fish teeth (Lécuyer et al., 2003).

supported by both first-order high sea level at a large scale (West Tethyan domain); (Hardenbol et al., 1998; Jacquin and de Graciansky, 1998) as well as the disappearance of glendonites balanced by appearance of tillites and dropstones in high latitudes around the Oxfordian–Kimmeridgian transition (Price, 1999). A 1‰ decrease of $\delta^{18}O_{seawater}$ due to ice sheets would correspond to around 100 m on sea-level variation with Pleistocene glacial–interglacial change as reference, which is coherent with that observed at a large scale from the Late Oxfordian to the Early Kimmeridgian (Hardenbol et al., 1998; Jacquin and de Graciansky, 1998). In the Paris Basin, a significant sea-level rise is evidenced by the transition between lagoonal limestones and lower offshore Early Kimmeridgian clay formations, although it remains difficult to quantify. Part of the oyster shell $\delta^{18}O$ decrease between the Late Oxfordian and the Early Kimmeridgian may have been partly induced by a decrease of evaporation rates, since the depositional setting evolves from lagoon to outer ramp environments. However, as there is no sedimentological evidence to support high salinity episodes throughout this interval, we favour polar ice waning as the most likely factor to have induced a decrease of seawater oxygen isotope composition.

The revised temperatures estimated from the oyster shell $\delta^{18}O$ values (this study) compare well with estimates derived from fish tooth $\delta^{18}O$ values from comparable latitudes (Paris Basin, Subalpine Basin and Jura Mountains; Fig. 5). This highlights the reliability of oyster shell $\delta^{18}O$ values for paleotemperature reconstructions. Our work based on numerous and stratigraphically well-dated samples allow us to improve the previously published isotopic temperature history (Jenkyns et al., 2002; Lécuyer et al., 2003). More specifically, we identify a warming episode in the early Middle Oxfordian (*plicatilis* Zone), followed by cooling in the Late Oxfordian (*bifurcatus–bimmamatum* Zones). The Middle Oxfordian warming is supported by 1) the appearance of coral reefs in eastern Paris Basin (Carpentier et al., 2006; Cecca et al., 2005), 2) a northern migration of Boreal ammonites in the western Tethyan realm starting in the *plicatilis* Zone (Carpentier et al., 2006; Cecca et al., 2005), 3) a migration event of Mediterranean ammonites (genus *Platysphinctes*) into the Polish Jura Chain (Sub-Mediterranean Province) in the *plicatilis* Zone (Głowniak, 2000), 4) a change in the spore and pollen association occurring during this time interval (*densiplicatum* Zone) in the area of the North Sea indicating drier conditions (Abbink et al., 2001) and 5) a change in vascular plant biomarkers in the Paris Basin (Hautevelle et al., 2006) also indicating drier conditions. The following cooler episode in the *bifurcatus–bimmamatum* Zones agrees well with i) a decrease in coral diversity in Lorraine (eastern Paris Basin); (Carpentier et al., 2006), ii) Boreal *Amoeboceras* invasions into the Polish Jura Chain in the *bimmamatum* Zone (Matyja and Wierzbowski, 2000) and iii) a change in the sporomorph association in the North Sea (*Regular* Zone, Late Oxfordian); (Abbink et al., 2001).

The consequent observed warming in the late Late Oxfordian to Kimmeridgian is supported by oxygen isotope ratios of i) bivalve shells from England (Jenkyns et al., 2002; Malchus and Steuber, 2002), (Fig. 5) and ii) nannofossils from the Germanic Sea which indicate a warming of 8 °C in the *bifurcatus* to *Platynota* Zone (Late Oxfordian) (Bartolini et al., 2003). A similar warming trend for the Oxfordian was previously reported based on $\delta^{18}O$ values of brachiopod shells from the eastern Paris Basin (Carpentier et al., 2006) that were recovered from the same outcrop than the oyster shells analysed in our study. However, temperatures inferred from $\delta^{18}O$ of brachiopod shell calcite are systematically higher by on average 6 °C in comparison to paleotemperatures inferred from $\delta^{18}O$ of oyster shell calcite and fish tooth apatite (Lécuyer et al., 2003); Fig. 5. Both diagenesis as well as vital fractionation effects can lower $\delta^{18}O$ values of shell calcite. It is generally assumed that brachiopod calcite is precipitated in oxygen isotopic equilibrium with seawater (Brand et al., 2003), although a recent study on the modern brachiopod *T. transversa* has shown that the secondary shell layer exhibits a strong kinetic fractionation resulting in an offset from expected equilibrium values as large as 4‰, representing an error of about 16 °C on calculated seawater temperatures (Auclair et al., 2003). The observed 1.5‰ offset in the oxygen isotope composition of brachiopod and oyster shell calcite may be explained by non-equilibrium fractionation during the precipitation of brachiopod shell calcite. Nevertheless, if there is a systematic offset between the $\delta^{18}O$ of oyster shells and brachiopods, they both show the same relative evolution throughout the Oxfordian–Kimmeridgian interval. The more numerous brachiopod data during the *transversarium* Zone point to a temperature maximum spanning most of this interval, with an abrupt cooling at the *transversarium/bifurcatus* boundary.

Temperatures calculated from $\delta^{18}O$ of belemnites of the Polish Jura Chain, Kujawy area (Poland), Swabian Alb (Germany), England, Russia and Isle of Skye (Scotland) range from 12 to 20 °C (Jenkyns et al., 2002; Jones et al., 1994; Podlaha et al., 1998; Wierzbowski, 2002, 2004); (using a $\delta^{18}O_{seawater}$ of −1‰ for temperature calculation, as belemnites are thought to live both in deeper marine environments (Wierzbowski, 2002; Wierzbowski, 2004; Wierzbowski and Joachimski, 2007) and as these belemnites lived at higher latitudes than the Paris Basin) and are significantly colder than temperatures estimated for the eastern Paris Basin. In addition, these temperatures calculated from belemnites do not define a clear trend within the Oxfordian–Early Kimmeridgian interval but rather exhibit limited variations throughout this time interval, except for belemnites from Russia and England that define a warming trend in the *plicatilis* Zone. The colder and quite stable temperatures calculated from the belemnites from Poland, Germany and Scotland could be explained by the position of Scotland at higher latitudes during the Oxfordian and potentially by a deeper water habitat of Submediterranean and Mediterranean belemnites (Wierzbowski, 2004).

6. Conclusions

Oxygen isotope ratios measured on biostratigraphically well-dated oyster shells provide new insights in the evolution of SST in the western Tethys during the Oxfordian–Early Kimmeridgian. Best estimates of reconstructed paleotemperatures point to a climatic warming of 3 °C from the *cordatum* to *transversarium* Zone, followed by cooling of 7 °C with minimum temperatures recorded within the *bimmamatum* Zone. Another warming of 7 °C is suggested for the *bimmamatum* and *cymodoce* Zone. Intra-shell $\delta^{18}O$ variations suggest minimum estimates of seasonal SST variations from about 2 °C for the deepest environments to about 5 °C on average for the shallowest environments during the Oxfordian–Early Kimmeridgian interval. Our new data are in agreement with fish tooth $\delta^{18}O$ data (Lécuyer et al., 2003; Picard et al., 1998), but yield lower temperatures than co-occuring brachiopods (Carpentier et al., 2006).

Acknowledgements

We thank Fabrice Monna for assistance in statistically treatment of data, Jacques Thierry for advices concerning the ammonite Zone correlations, Daniele Lutz and Pascal Taubaty for assistance in the laboratory. Hubert Wierzbowski and two anonymous reviewers are thanked for their helpful comments.

Appendix A. Supplementary data

Supplementary data associated with this article can be found, in the online version, at doi:10.1016/j.epsl.2008.06.015.

References

Abbink, O., Targarona, J., Brinkhuis, H., Visscher, H., 2001. Late Jurassic to earliest Cretaceous palaeoclimatic evolution of the southern North Sea. Glob. Planet. Change 30, 231–256.
Anderson, T.F., Arthur, M.A., 1983. Stable isotopes of oxygen and carbon and their application to sedimentologic and paleonvironmental problems. In: Arthur, M.A., Anderson, T.F., Kaplan, I.R., Veizer, J., Land, L.S. (Eds.), Stable Isotopes in Sedimentary Geology. Society of Economic Paleontologists and Mineralogists Short Course, vol. 10, pp. 1–151.
Auclair, A.-C., Joachimski, M.M., Lécuyer, C., 2003. Deciphering kinetic, metabolic and environmental controls on stable isotope fractionations between seawater and the shell of *Terebratalia transversa* (Brachiopoda). Chem. Geol. 202, 59–78.
Bartolini, A., Pittet, B., Mattioli, E., Hunziker, J.C., 2003. Shallow-platform palaeoenvironmental conditions recorded in deep-shelf sediments: C and O stable isotopes in Upper Jurassic sections of southern Germany (Oxfordian–Kimmeridgian). Sediment. Geol. 160, 107–130.
Brand, U., Logan, A., Hiller, N., Richardson, J., 2003. Geochemistry of modern brachiopods: applications and implications for oceanography and paleoceanography. Chem. Geol. 198, 305–334.
Carpentier, C., Martin-Garin, B., Lathuilière, B., Ferry, S., 2006. Correlation of reefal Oxfordian episodes and climatic implications in the eastern Paris Basin (France). Terra Nova 18, 191–201.
Carpentier, C., Lathuiliere, B., Ferry, S., Sausse, J., 2007. Sequence stratigraphy and tectonosedimentary history of the Upper Jurassic of the Eastern Paris Basin (Lower and Middle Oxfordian, northeastern France). Sediment. Geol. 197, 235–266.
Cecca, F., Martin Garin, B., Marchand, D., Lathuiliere, B., Bartolini, A., 2005. Paleoclimatic control of biogeographic and sedimentary events in Tethyan and peri-Tethyan areas during the Oxfordian (Late Jurassic). Palaeogeogr. Palaeoclimat. Palaeoecol. 222, 10–32.
Debrant-Passard, S., Enay, R., Rioult, M., Cariou, E., Marchand, D., Menot, J.-C., 1980. 6: Jurassique supérieur. In: Megnien, C. (Ed.), Synthèse géologique du Bassin de Paris. Vol. Mémoire BRGM, vol. 101. BRGM, p. 470.
Dromart, G., Garcia, J.-P., Gaumet, F., Picard, S., Rousseau, M., Atrops, F., Lecuyer, C., Sheppard, S.M.F., 2003a. Perturbation of the carbon cycle at the middle/Late Jurassic transition: geological and geochemical evidence. Am. J. Sci. 303, 667–707.
Dromart, G., Garcia, J.P., Picard, S., Atrops, F., Lécuyer, C., Sheppard, S.M.F., 2003b. Ice age at the Middle–Late Jurassic transition? Earth Planet. Sci. Lett. 213, 205–220.

Enay, R., Boullier, A., 1981. L'âge du complexe récifal des côtes de Meuse entre Verdun et Commercy et la stratigraphie de l'Oxfordien dans l'Est du bassin de Paris. Géobios 14, 727–771.

Fairbanks, R.G., Charles, C.D., Wright, J.D., 1992. Origin of global meltwater pulses. In: Taylor, R.E.e.a. (Ed.), Radiocarbon After Four Decades. An Interdisciplinary Perspective. Springer, pp. 473–500.

Frakes, L.A., Francis, J.E., Syktus, J.I., 1992. Climate Modes of the Phanerozoic. Cambridge Univ. Press, New York.

Głowniak, E., 2000. The Platysphinctes immigration event in the Middle Oxfordian of the Polish Jura Chain (Central Poland). Acta Geol. Pol. 50, 143–160.

Głowniak, E., 2005. The Wartae Subzone — a proposal for the lower boundary of the unified Upper Oxfordian Substage in the Submediterranean Province. ISJS Newsletter, vol. 32, pp. 34–37.

Głowniak, E. and Wierzbowski, H., 2007. Comment on "The mid-Oxfordian (Late Jurassic) positive carbon-isotope excursion recognised from fossil wood in the British Isles" by C.R. Pearce, S.P. Hesselbo, A.L. Coe, Palaeogeography, Palaeoclimatology, Palaeoecology 221: 343–357. Palaeogeography, Palaeoclimatology, Palaeoecology. 248, 247–251.

Gradstein, F.M., Ogg, J.G., Smith, A.G., 2004. A Geological Time Scale 2004. Cambridge University Press.

Gygi, R.A., Coe, A.L., Vail, P.R., 1998. Sequence stratigraphy of the Oxfordian and Kimmeridgian stages (Late Jurassic) in Northern Switzerland. SEPM Spec. Publ. 60, 527–544.

Hallam, A., 1993. Jurassic climates as inferred from the sedimentary and fossil record. Philos. Trans. - R. Soc. Lond. 341, 287–293.

Hardenbol, J., Thierry, J., Farley, M.B., Jacquin, T., Graciansky, P.-C.D., Vail, P.R., 1998. Mesozoic and Cenozoic sequence chronostratigraphy framework of European Basins. In: de Graciansky, C., Hardenbol, J., Jacquin, T., Vail, P.R. (Eds.), Mesozoic and Cenozoic Sequence Stratigraphy of European Basins. SEPM Special Publication, vol. 60.

Hautevelle, Y., Michels, R., Malartre, F., Trouiller, A., 2006. Vascular plant biomarkers as proxies for Palaeoflora and palaeoclimatic changes at the Dogger/Malm transition of the Paris Basin (France). Org. Geochem. 37, 610–625.

Jacquin, T., de Graciansky, P.-C., 1998. Major transgressive/regressive cycles: the stratigraphic signature of European Basin development. In: de Graciansky, C., Hardenbol, J., Jacquin, T., Vail, P.R. (Eds.), Mesozoic and Cenozoic Sequence Stratigraphy of European Basins. Vol. SEPM Special publication, vol. 60, pp. 15–29.

Jenkyns, H.C., Jones, C.E., Grocke, D.R., Hesselbo, S.P., Parkinson, D.N., 2002. Chemostratigraphy of the Jurassic System: applications, limitations and implications for palaeoceanography. J. Geol. Soc. 159, 351–378.

Jones, C.E., Jenkins, H.C., Coe, A.L., Hesselbo, S.P., 1994. Strontium isotopic variations in Jurassic and Cretaceous sea-water. Geochim. Cosmochim. Acta 58, 3061–3074.

Lathuilière, B., Gaillard, C., Habrant, N., Bodeur, Y., Boullier, A., Enay, R., Hanzo, M., Marchand, D., Thierry, J., Werner, W., 2005. Coral zonation of an Oxfordian reef tract in the northern French Jura. Facies 50, 545–559.

Lécuyer, C., Picard, S., Garcia, J.-P., Sheppard, S.M.F., Grandjean, P., Dromart, G., 2003. Thermal evolution of Tethyan surface waters during the Middle–Late Jurassic: evidence from D18O values of marine fish teeth. Paleoceanography 18.

Lécuyer, C., Reynard, B., Martineau, F., 2004. Stable isotope fractionation between mollusc shells and marine waters from Martinique Island. Chem. Geol. 213, 293–305.

Levitus, S. and Boyer, T., 1994. World Ocean Atlas 1994. NOAA Atlas NESDIS 4, U.S. Dept. Commerce. http://www.ingrid.ldeo.columbia.edu/SOURCES/.LEVITUS94/.

Levitus, S., Burgett, R. and Boyer, T., 1994. World Ocean Atlas 1994. NOAA Atlas NESDIS 3 US Dept. Commerce. http://www.ingrid.ldeo.columbia.edu/SOURCES/.LEVITUS94/.

Malchus, N., Steuber, T., 2002. Stable isotope records (O, C) of Jurassic aragonitic shells from England and NW Poland: palaeoecologic and environmental implications. Géobios 35, 29–39.

Matyja, B.A., Wierzbowski, A., 1997. The quest for unified Oxfordian/Kimmeridgian boundary: implications of the ammonite succession at the turn of the Bimammatum and Planula zones in the Wieluń upland, Central Poland. Acta Geol. Pol. 47, 77–105.

Matyja, B.A., Wierzbowski, A., 1998. The stratigraphy and palaeogeographical importance of the Oxfordian and Lower Kimmeridgian succession in the Kcynia IG IV borehole (in Polish). Biuletyn PIG 382.

Matyja, B.A., Wierzbowski, A., 2000. Biological response of ammonites to changing environmental conditions: an example of Boreal Amoeboceras invasions into Submediterranean Province during Late Oxfordian. Acta Geol. Pol. 50, 45–54.

Matyja, B.A., Wierzbowski, A., Wright, J.K., 2006. The Subboreal/Boreal ammonite succession at the Oxfordian/Kimmeridgian boundary at Flodigarry, Staffin Bay (Isle Of Skye), Scotland. Trans. R. Soc. Edinb. Earth Sci. 96, 387–405.

McArthur, J.M., Doyle, P., Leng, M.J., Reeves, K., Williams, T., Garcia-Sanchez, R., Howarth, R.J., 2007. Testing palaeo-environmental proxies in Jurassic belemnites: Ca/Mg, Sr/Mg, Na/Mg, d13C and d18O. Palaeogeogr. Palaeoclimatol. Palaeoecol. 252, 464–480.

Mook, W.G., Vogel, J.C., 1968. Isotopic equilibrium between shells and their environment. Science 159, 874–875.

Olivier, N., Carpentier, C., Martin-Garin, B., Lathuilière, B., Gaillard, C., Ferry, S., Hantzpergue, P., Geister, J., 2004. Coral-microbialite reefs in pure carbonate versus mixed carbonate-siliciclastic depositional environments: the example of the Pagny-sur-Meuse section (Upper Jurassic, Northeastern France). Facies. 50, 229–255.

Pearce, C.R., Hesselbo, S.P., Coe, A.L., 2005. The mid-Oxfordian (Late Jurassic) positive carbon-isotope excursion recognised from fossil wood in the British Isles. Palaeogeogr. Palaeoclimatol. Palaeoecol. 221, 343–357.

Picard, S., Garcia, J.P., Lécuyer, C., Sheppard, S.M.F., Cappetta, H., Emig, C.C., 1998. $\delta^{18}O$ values of coexisting brachiopods and fish: temperature differences and estimates of paleo-water depths. Geology 26, 975–978.

Podlaha, O.G., Muterlose, J., Veizer, J., 1998. Preservation of delta O-18 and delta C-13 in belemnite rostra from the Jurassic Early Cretaceous successions (vol 298, pg 324, 1998). Am. J. Sci. 298 534–534.

Price, G.D., 1999. The evidence and implications of polar ice during the Mesozoic. Earth-Sci. Rev. 48, 183–210.

Pucéat, E., Lécuyer, C., Sheppard, S.M.F., Dromart, G., Reboulet, S., Grandjean, P., 2003. Thermal evolution of Cretaceous Tethyan marine waters inferred from oxygen isotope composition of fish tooth enamels. Paleoceanography 18, 1029–1040.

Pucéat, E., Lécuyer, C., Donnadieu, Y., Naveau, P., Cappetta, H., Ramstein, G., Huber, B.T., Kriwet, J., 2007. Fish tooth delta 18O revising Late Cretaceous meridional upper ocean water temperature gradients. Geology 35, 107–110.

Riboulleau, A., Baudin, F., Daux, V., Hantzpergue, P., Renard, M., Zakharov, V., 1998. Evolution de la paléotempérature des eaux de la plate-forme russe au cours du Jurassique supérieur. C. R. Acad. Sci. 326, 239–246.

Roche, D.M., Donnadieu, Y., Pucéat, E., Paillard, D., 2006. Effect of changes in delta O-18 content of the surface ocean on estimated sea surface temperatures in past warm climate. Paleoceanography 21.

Schweigert, G., Callomon, J.H., 1997. Der bauhini-Faunenhorizont und seine Bedeutung fur die Korrelation zwischen tethyalem und subborealem Oberjura. Stuttg. Beitr. Naturkd. 247, 1–69.

Sellwood, B., Valdes, P., 1997. Geological evaluation of climate General Circulation Models and model implications for Mesozoic cloud cover. Terra Nova 9, 75–78.

Sellwood, B., Valdes, P., Price, G., 2000. Geological evaluation of multiple general circulation model simulations of Late Jurassic palaeoclimate. Palaeogeogr. Palaeoclimatol. Palaeoecol. 156, 147–160.

Shackleton, N.J., Kennet, D.J., 1975. Paleotemperature history of the Cenozoic and initiation of Antarctic glaciation: oxygen and carbon isotope analyses in DSDP sites 277, 279 and 289. Init. Rep. Deep Sea Drill. Proj. 29, 743–755.

Steuber, T., Rauch, M., Masse, J.P., Graaf, J., Malkoc, M., 2005. Low-latitude seasonality of Cretaceous temperatures in warm and cold episodes. Nature. 437, 1341–1344.

Surge, D., Lohmann, K.C., Dettman, D.L., 2001. Controls on isotopic chemistry of the American oyster, *Crassostrea virginica*: implications for growth patterns. Palaeogeogr. Palaeoclimat. Palaeoecol. 172, 283–296.

Thierry, J., 2000. Early Kimmeridgian. Map 10. In Dercourt, J., Gaetani, M., Vrielynck, B., Barrier, E., Biju-Duval, B., Brunet, M.F., Cadet, J.P., Crasquin, S. and Sandulescu, M. (Eds.), Atlas Peri-Tethys. Palaeogeographical Maps.

Tucker, M.E., Wrigth, V.P., 1990. Carbonate Sedimentology. Blackwell, Oxford.

Vincent, B., 2001. Sédimentologie et Géochimie de la Diagenèse des carbonates. Application au Malm de la bordure Est du Bassin de Paris. Centre des Sciences de la Terre. University of Burgundy, Dijon, p. 380.

Vincent, B., Rambeau, C., Emmanuel, L., Loreau, J.-P., 2006. Sedimentology and trace element geochemistry of shallow-marine carbonates: an approach to paleoenvironmental analysis along the Pagny-sur-Meuse Section (Upper Jurassic, France). Facies 52, 69–84.

Weissert, H., Mohr, H., 1996. Late Jurassic climate and its impact on carbon cycling. Palaeogeogr. Palaeoclimat. Palaeoecol. 122, 27–43.

Wierzbowski, H., 2002. Detailed oxygen and carbon isotopic stratigraphy of the Oxfordian in Central Poland. Int. J. Earth. Sci. 91, 304–314.

Wierzbowski, H., 2004. Carbon and oxygen isotope composition of Oxfordian–Early Kimmeridgian belemnite rostra: palaeoenvironmental implications for Late Jurassic seas. Palaeogeogr. Palaeoclimatol. Palaeoecol. 203, 153–168.

Wierzbowski, H., Joachimski, M., 2007. Reconstruction of late Bajocian–Bathonian marine palaeoenvironments using carbon and oxygen isotope ratios of calcareous fossils from the Polish Jura Chain (central Poland). Palaeogeogr. Palaeoclimatol. Palaeoecol. 254, 523–540.